Noradrenaline inhibits exocytosis via the G protein $\beta\gamma$ subunit and refilling of the readily releasable granule pool via the $\alpha_{i1/2}$ subunit

Ying Zhao[1,2], Qinghua Fang[2], Susanne G. Straub[1], Manfred Lindau[2] and Geoffrey W. G. Sharp[1]

[1] *Department of Molecular Medicine, Cornell University, Ithaca, NY 14853, USA*
[2] *School of Applied and Engineering Physics, Cornell University, Ithaca, NY 14853, USA*

The molecular mechanisms responsible for the 'distal' effect by which noradrenaline (NA) blocks exocytosis in the β-cell were examined by whole-cell and cell-attached patch clamp capacitance measurements in INS 832/13 β-cells. NA inhibited Ca^{2+}-evoked exocytosis by reducing the number of exocytotic events, without modifying vesicle size. Fusion pore properties also were unaffected. NA-induced inhibition of exocytosis was abolished by a high level of Ca^{2+} influx, by intracellular application of antibodies against the G protein subunit Gβ and was mimicked by the myristoylated $\beta\gamma$-binding/activating peptide mSIRK. NA-induced inhibition was also abolished by treatment with BoNT/A, which cleaves the C-terminal nine amino acids of SNAP-25, and also by a SNAP-25 C-terminal-blocking peptide containing the BoNT/A cleavage site. These data indicate that inhibition of exocytosis by NA is downstream of increased $[Ca^{2+}]_i$ and is mediated by an interaction between G$\beta\gamma$ and the C-terminus of SNAP-25, as is the case for inhibition of neurotransmitter release. Remarkably, in the course of this work, a novel effect of NA was discovered. NA induced a marked retardation of the rate of refilling of the readily releasable pool (RRP) of secretory granules. This retardation was specifically abolished by a G$\alpha_{i1/2}$ blocking peptide demonstrating that the effect is mediated via activation of Gα_{i1} and/or Gα_{i2}.

(Received 15 March 2010; accepted after revision 14 July 2010; first published online 19 July 2010)
Corresponding author G. W. G. Sharp: Department of Molecular Medicine, Cornell University, Ithaca, NY 14853-6401, USA. Email: gws2@cornell.edu

Abbreviations BoNT/A, botulinum toxin A; Im, imaginary part of the patch admittance; mSIRK, myristoylated $\beta\gamma$-binding/activating peptide; NA, noradrenaline; PTX, pertussis toxin; Re, real part of the patch admittance; RRP, readily releasable pool; SNAP-25, synaptosomal-associated protein 25; SNARE, SNAP (soluble NSF attachment protein) receptors.

Introduction

In pancreatic β-cells, a variety of inhibitory agonists, such as NA, somatostatin and PGE_1 reduce insulin secretion via activation of G protein-coupled receptors (Sharp, 1996). This inhibition of insulin release is sensitive to pertussis toxin (PTX), indicating the involvement of heterotrimeric G_i and/or G_o proteins (Katada & Ui, 1979; Komatsu *et al.* 1995*a*). The mechanisms of G_i/G_o-mediated inhibition include the activation of K_{ATP} channels and inhibition of adenylyl cyclase, and a so-called 'distal action' at a point late in stimulus–secretion coupling (Sharp, 1996; Lang, 1999). The latter, which occurs downstream of increased $[Ca^{2+}]_i$ and blocks exocytosis *per se*, is the most powerful of the individual inhibitory mechanisms (Sharp *et al.* 1989; Drews *et al.* 1994; Komatsu *et al.* 1995*b*). Studies on the mechanism of serotonin-mediated inhibition of the presynaptic synapse in the lamprey (Blackmer *et al.* 2001; Gerachshenko *et al.* 2005) and on permeabilized PC12 cells (Blackmer *et al.* 2005) have shown that G$\beta\gamma$ subunits bind to synaptosomal-associated protein 25 (SNAP-25) and impair vesicle fusion mediated by the SNARE ('SNAP (soluble NSF attachment protein) receptors') complex. However, in insulin-secreting cells it has been proposed that the protein phosphatase calcineurin mediates the distal inhibition (Renstrom *et al.* 1996). In view of the evidence that the inhibition of neurotransmitter release downstream of increased $[Ca^{2+}]_i$ is due to the interaction of G$\beta\gamma$ with the SNARE complex and blockade of synaptotagmin binding, we investigated the possibility that this mechanism was also operative in the β-cell. In doing so, we found that G$\beta\gamma$ is indeed the mediator of the distal effect and that inhibition is due to a reduction in the number of exocytotic events without any change in

 DOI: 10.1113/jphysiol.2010.190090

vesicle size. Moreover, we also uncovered a novel effect of noradrenaline, namely to slow the refilling of the RRP.

Methods

Cell culture

INS 832/13 beta-cells (a kind gift of Dr C. B. Newgard) were cultured in complete RPMI-1640 medium supplemented with 10% fetal bovine serum, 100 μg ml^{-1} streptomycin, and 100 U ml^{-1} penicillin at 37°C in a 95% air–5% CO_2 atmosphere. The cells (passage numbers 60–66) were divided once a week by treatment with trypsin and the medium was changed twice between divisions. The measurements were performed 1–2 days after cell plating.

Whole-cell patch-clamp and capacitance measurements

Data were acquired using a PULSE 8.75-controlled EPC-10 amplifier (HEKA electronics). Exocytosis was elicited by voltage-clamp depolarizations (from −70 mV to +10 mV, the pulse duration and pulse frequencies varied according to the different stimulation protocols) and detected as changes in cell capacitance estimated by the Lindau–Neher technique as implemented by the 'Sine+DC' feature of the lock-in software module (sine wave stimulus: 500 Hz, 40 mV peak-to-peak amplitude, DC-holding potential −70 mV). The membrane capacitance (C_m) was analysed with the customized IgorPro routines (WaveMetrics). The standard extracellular solution contained (in mM): 120 NaCl, 20 TEA-Cl, 2.6 $CaCl_2$, 5.6 KCl, 1.2 $MgCl_2$, 10 glucose and 10 Hepes-NaOH (pH 7.4). The pipette solution contained (in mM): 145 caesium glutamate, 8 NaCl, 0.18 $CaCl_2$, 0.28 BAPTA, 1 $MgCl_2$, 2 ATP-Mg, 0.5 GTP-Na_2, 0.3 cAMP, 10 Hepes-CsOH (pH 7.3), and 300 nM calculated free $[Ca^{2+}]_i$. Na^+ currents were blocked by 500 nM TTX. NA was freshly prepared before experiments and added into the extracellular solution at a final concentration of 5 μM. mSIRK (Calbiochem Corporation) was dissolved in DMSO and stored at −20°C as stock. The antibodies of Gβ and G$\alpha_{i,o,t,z,gust}$ used in the studies were purchased from Santa Cruz Biotechnology, Inc. (Santa Cruz, CA, USA). The peptides containing the same sequences as the last 13 amino acids of the C-termini of G$\alpha_{i1/2}$, Gα_{i3}, Gα_{o1}, Gα_{o2} and scrambled peptide (as control) were purchased from GenScript Corporation and had greater than 90% purity. They were dissolved in ddH_2O and stored at −20°C as stocks and added to the pipette solutions at a concentration of 60 μM on the day of the experiments. Botulinum toxin A (BoNT/A) light chain was purchased from List Biological Laboratories, Inc. It was dissolved in intracellular solution at a final concentration of 1 μM. Before stimulation, ∼5 min was allowed for the antibodies, peptides or BoNT/A light chain to reach the equilibrium between the pipette solution and cytosol. The recordings were performed at temperatures between 32 and 35°C.

Cell-attached capacitance measurements

After wax-coating and fire-polishing, the pipette tips had resistances of >1 MΩ when filled with pipette solution containing (in mM): 50 NaCl, 100 TEA-Cl, 5 KCl, 1 $MgCl_2$, 5 $CaCl_2$, 10 Hepes-NaOH (pH 7.3). The cells were plated on an 8 mm coverslip and continuously bathed in a ∼70 μl solution containing (in mM): 130 NaCl, 5 KCl, 1 $MgCl_2$, 5 $CaCl_2$, 10 glucose, and 10 Hepes-NaOH (pH 7.3). The holding potential 0 mV was added to the sine wave (50 mV r.m.s., 20 kHz) from the lock-in amplifier and fed into the stimulus input of the patch-clamp amplifier. The C-slow compensation of the EPC-7 (HEKA electronics) was set to 0.2 pF, the G-series compensation to 0.2 pS. The pipette current was filtered by the built-in 10 kHz filter of the patch-clamp amplifier and scaled down by a factor of 10 before input to the lock-in amplifier. The correct phase for the lock-in amplifier was found by utilizing a capacitance dither switch on the patch-clamp amplifier. At the correct phase, the lock-in amplifier computed the real (Re) and the imaginary part (Im) of the pipette current, which was recorded by the 16-bit ADC as Y1 and Y2, respectively. The output filter of the lock-in amplifier was set to 1 ms time constant, 24 dB octave^{-1}. After the recording, the calibration pulses were used to convert units of the Y1 and Y2 traces from raw counts into pS and fF, respectively. Individual vesicle capacitance step size values were converted to vesicle diameters assuming spherical geometry and a specific vesicle capacitance of 9 fF μm^{-2}.

Data analysis

To minimize the variations due to different cell sizes, all the ΔC_m values were normalized by the cell sizes (fF pF^{-1}). Data are presented as means ± S.E.M. Significance was determined either by Student's *t* test or by ANOVA followed by Fisher's least significant difference test as appropriate.

Results

Increased Ca^{2+} entry abolishes the inhibitory effects of NA on insulin exocytosis

In the whole-cell patch-clamp configuration (Lindau & Neher, 1988), exocytosis was stimulated by depolarizing pulses (from −70 mV to +10 mV) in INS 832/13 cells and was identified as the capacitance increase of cell membrane (ΔC_m). The NA-mediated inhibition of insulin secretion was evaluated by monitoring ΔC_m in response

to varying pulse durations at a constant extracellular Ca^{2+} concentration ($[Ca^{2+}]_o$) of 2.6 mM. The test cells were incubated in extracellular solution containing NA for ~2–5 min before the recordings. The averaged traces of ΔC_m and I_{Ca}, evoked by depolarizing pulses with different durations (100, 300 and 500 ms) in control and NA-treated cells, are presented in Fig. 1*A*, *B* and *C*. Ca^{2+} currents were recorded while the capacitance measurements were interrupted and Ca^{2+} entry was quantified by the Ca^{2+} current integral. The absolute values of ΔC_m (fF) and of charge integrals (pQ) were normalized by cell size (pF) and defined as fF pF^{-1} and pQ pF^{-1}, respectively. When

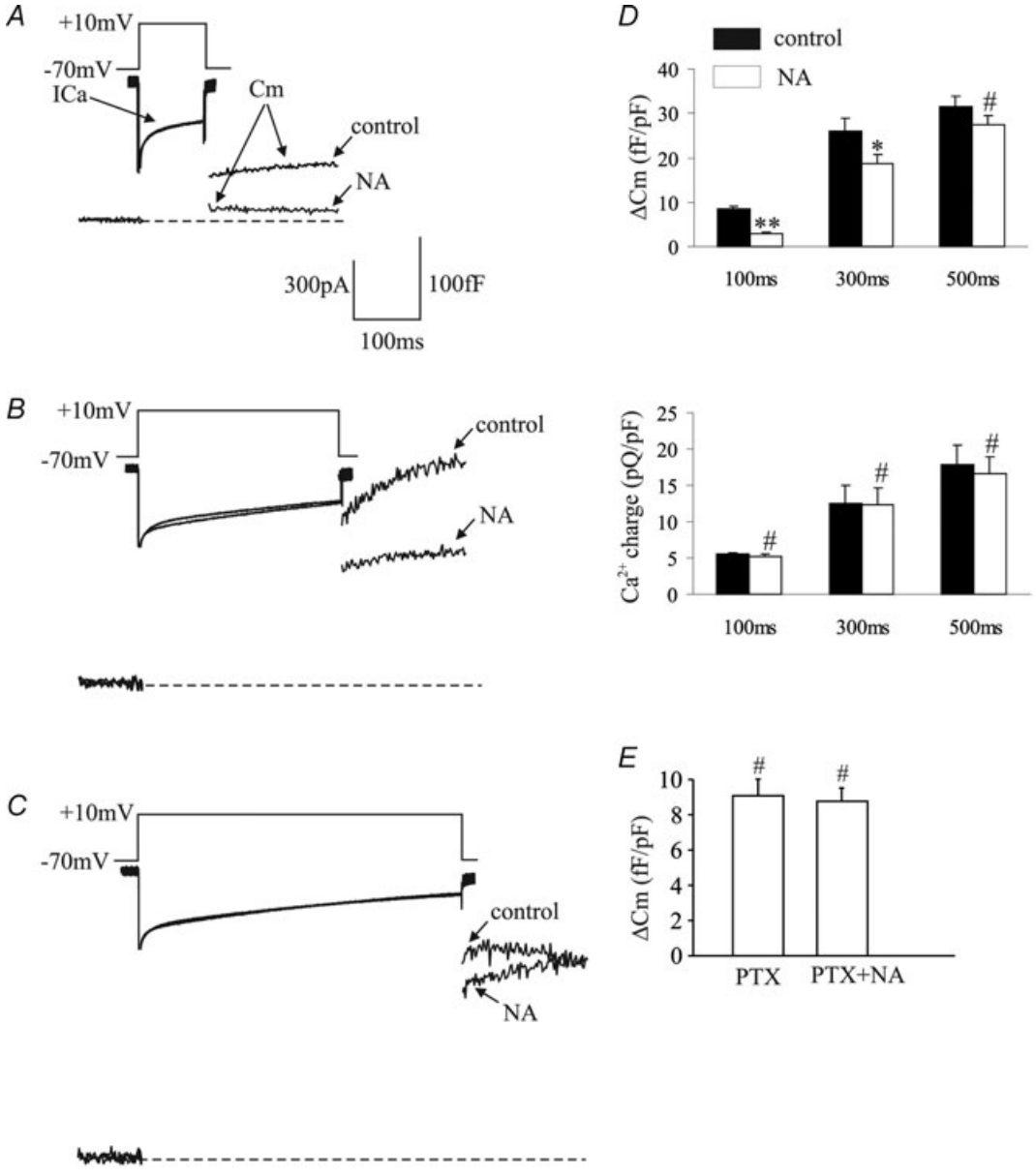

Figure 1. Increasing the Ca^{2+} influx by the prolongation of the depolarizing pulse can alleviate and/or abolish the inhibitory effects of NA on exocytosis

Using standard whole-cell capacitance measurements, the exocytosis elicited by depolarizing pulses (from −70 mV to +10 mV) with various pulse durations was monitored in control and hormone-treated cells. During the depolarizing pulses, the Ca^{2+} currents were recorded simultaneously. *A*, *B* and *C*, the recording traces of capacitance and I_{Ca} in control and NA-treated cells stimulated with 100, 300 and 500 ms pulses, respectively. *D*, the summaries of capacitance changes (upper) and calcium influxes (lower) in *A*, *B* and *C*, control (filled columns) and NA (open columns). *E*, the summaries of the capacitance changes on PTX-treated cells. In *A*, *B* and *C*, the arrows indicate I_{Ca}, C_m and the different experimental conditions. The traces shown in the figure were averaged from 14–41 cells. In *D* and *E* the values of ΔC_m and charge integrals were normalized by cell size (fF pF^{-1} and pQ pF^{-1}). $^*P < 0.05$, $^{**}P < 0.01$, #n.s.

pulses of increasing duration were used to stimulate the cells, such that Ca^{2+} entry was progressively increased, a parallel increase in exocytosis was observed. As shown in the statistical analysis (Fig. 1*D*, upper panel), with a pulse duration of 100 ms (Fig. 1*A*), NA exhibited strong inhibition of exocytosis (control, 8.5 ± 0.6 fF pF^{-1}, $n = 41$ cells; NA, 2.8 ± 0.3 fF pF^{-1}, $n = 30$ cells, $P < 0.01$, ~67% inhibition). With a longer pulse of 300 ms (Fig. 1*B*) a larger increase in exocytosis occurred but the inhibitory effect of NA was significantly reduced (control, 25.9 ± 2.9 fF pF^{-1}, $n = 15$ cells; NA, 18.7 ± 1.9 fF pF^{-1}, $n = 14$ cells, $P < 0.05$, ~28% inhibition). When the pulse duration was prolonged up to 500 ms, such that Ca^{2+} entry was further increased, the ΔC_m in control cells was 31.6 ± 2.2 fF pF^{-1} ($n = 34$ cells), 3.7-fold greater than that seen with the 100 ms pulse ($P < 0.01$) and significantly greater than that of the 300 ms pulse ($P < 0.05$) (Fig. 1*D*). However, with the 500 ms pulse, NA-induced inhibition of exocytosis was abolished (NA, 27.4 ± 2.0 fF pF^{-1}, $n = 28$ cells, n.s.). Ca^{2+} influx was strongly increased by the pulses of longer duration but was not affected by NA (Fig. 1*D*, lower panel) (control/NA, 100 ms: $5.5 \pm 0.3/5.2 \pm 0.4$ pQ pF^{-1}, n.s.; 300 ms: $12.5 \pm 2.5/12.4 \pm 2.3$ pQ pF^{-1}, n.s.; 500 ms: $17.8 \pm 2.7/16.6 \pm 2.4$ pQ pF^{-1}, n.s.). These results indicate that the inhibitory effect of NA on insulin secretion can be counteracted by a high level of Ca^{2+} entry. The effect of NA on exocytosis was mediated by activation of G_i/G_o proteins, since pretreatment of the cells with PTX (150 ng ml^{-1}, >24 h) abolished the inhibitory effects (PTX, 9.1 ± 1.1 fF pF^{-1}, $n = 12$ cells; PTX+NA, 8.8 ± 0.9 fF pF^{-1}, $n = 11$ cells, n.s.) (Fig. 1*E*).

In similar experiments designed to increase Ca^{2+} influx by increasing $[Ca^{2+}]_o$ at a fixed pulse duration of 100 ms, NA-induced inhibition of exocytosis was apparent at 1.1 mM (control, 4.7 ± 0.8 fF pF^{-1}, $n = 11$ cells; NA, 1.6 ± 0.3 fF pF^{-1}, $n = 14$ cells, $P < 0.05$) and 2.6 mM $[Ca^{2+}]_o$ (control, 7.0 ± 0.6 fF pF^{-1}, $n = 27$ cells; NA, 2.7 ± 0.4 fF pF^{-1}, $n = 32$ cells, $P < 0.01$) (Fig. 2*A*, *B* and *D*), but not at 10 mM $[Ca^{2+}]_o$ (control, 10.2 ± 1.5 fF pF^{-1}, $n = 18$ cells; NA, 9.0 ± 1.0 fF pF^{-1}, $n = 19$ cells, n.s.) and there was no effect of NA on Ca^{2+} influx (Fig. 2*C* and *D*) demonstrating again that a high Ca^{2+} influx blocks the inhibitory effect of NA.

NA inhibits insulin secretion by reducing the number of exocytotic events, without changing the size of exocytotic vesicles

To determine whether the change of capacitance was due to a decrease in exocytotic vesicle size or due to a reduction in the number of exocytotic events, cell-attached capacitance measurements were performed (Debus & Lindau, 2000). The cells were incubated in the extracellular solution containing 5 μM NA or without NA for ~5 min before the pipette was sealed onto a membrane patch, and the capacitance was recorded for ~10 min. Upward capacitance steps indicating individual exocytotic events were detected (see example in Fig. 3*A*, Im). Narrow, low conductance fusion pores lead to transient increases in the real part of the patch admittance (Fig. 3*A*, Re), which are evident for the larger events (e.g. Fig. 3*A*, left trace) but were usually undetectable for small events (e.g. Fig. 3*A*, right), presumably due to the low signal-to-noise ratio of these events, or due to a very rapid (<4.5 ms) increase of fusion pore conductance beyond our detection limit (Debus & Lindau, 2000). The mean step size and derived mean diameter of vesicles with a detectable change in the Re trace was ~0.8 fF (control, 0.81 ± 0.08 fF/172.2 ± 8.3 nm, 21.7% of the total events; NA, 0.82 ± 0.08 fF/174.1 ± 9.3 nm, 22.0%). The capacitance steps lacking a detectable transient in the Re trace had a mean size of ~0.5 fF (control, 0.52 ± 0.08 fF/137.6 ± 8.5 nm, 78.3%; NA, 0.53 ± 0.07 fF/138.9 ± 7.6 nm, 78.0%). NA reduced the number of exocytotic events per cell by ~65% (Fig. 3*B*), consistent with the ~70% inhibition observed in whole-cell recordings (Fig. 1*A*). The frequency distributions of exocytotic capacitance step size (Fig. 3*C*), as well as the mean values of the vesicle size (Fig. 3*D*) were similar in control and NA-treated conditions (control, 0.58 ± 0.10 fF/145.2 ± 11.2 nm, $n = 318$ events; NA, 0.59 ± 0.09 fF/146.7 ± 10.5 nm, $n = 227$ events, n.s.). Thus, inhibition of exocytosis by NA is due to a decrease in the number of events without a significant change in vesicle size and affects exocytotic vesicles of different sizes similarly. The diameter of most large dense core vesicles is >60 nm, and the corresponding capacitance step sizes are >0.1 fF (MacDonald *et al.* 2005), which is threefold larger than the peak-to-peak noise of our cell-attached capacitance measurements. The mean vesicle size of the control cells was slightly larger than that reported by MacDonald *et al.* The difference is probably due to the different lock-in amplifier filter applied. The lock-in amplifier setting used here (1 ms) allows a higher time resolution at the expense of a twofold higher recording noise. Therefore, the synaptic-like microvesicles, which produce small (0.01–0.1 fF) capacitance steps were not reliably detected due to the capacitance noise. Consequently, they were not included in the analysis here. However, the fast filter allowed us to detect the kinetics of the fusion pore. In cell-attached capacitance measurement, the fusion pore conductance and fusion pore lifetime provide information on fusion pore properties (Fang *et al.* 2008). As summarized from large events (Fig. 3*E* and *F*), control and NA-treated cells show similar mean values of fusion pore duration (control, 36.5 ± 7.8 ms, $n = 69$ events; NA, 40.1 ± 8.2 ms, $n = 50$ events, n.s.) and of the initial fusion pore

conductance (control, 0.28 ± 0.06 nS, $n = 69$ events; NA, 0.25 ± 0.08 nS, $n = 50$ events, n.s.). These data indicate that the fusion pore properties are not modulated by NA.

Inhibition of exocytosis by NA is mediated by G$\beta\gamma$ subunits

To test the possibility that in the β-cell the distal inhibition of exocytosis is mediated by G$\beta\gamma$ subunits, we used the cell-permeable myristoylated $\beta\gamma$-binding peptide mSIRK that promotes G protein subunit dissociation to release free $\beta\gamma$ subunits without activating the α subunits in intact cells (Goubaeva *et al.* 2003). In the whole-cell configuration, cells pretreated with mSIRK (30 μM, ~30 min) exhibited ~65% reduction of exocytosis (Fig. 4*Aa* and *b*), similar to that produced by NA (Fig. 1*A*) under the same stimulation protocol with 100 ms pulses (Fig. 4*Ab*, control, 10.7 ± 0.9 fF pF^{-1}, $n = 23$ cells; mSIRK, 3.9 ± 0.3 fF pF^{-1}, $n = 25$ cells, $P < 0.01$). Moreover, the inhibition induced by NA or mSIRK alone was not further enhanced by the combination of the two (Fig. 4*Ab*, NA+mSIRK, 4.0 ± 0.4 fF pF^{-1}, $n = 25$ cells, n.s.). To test

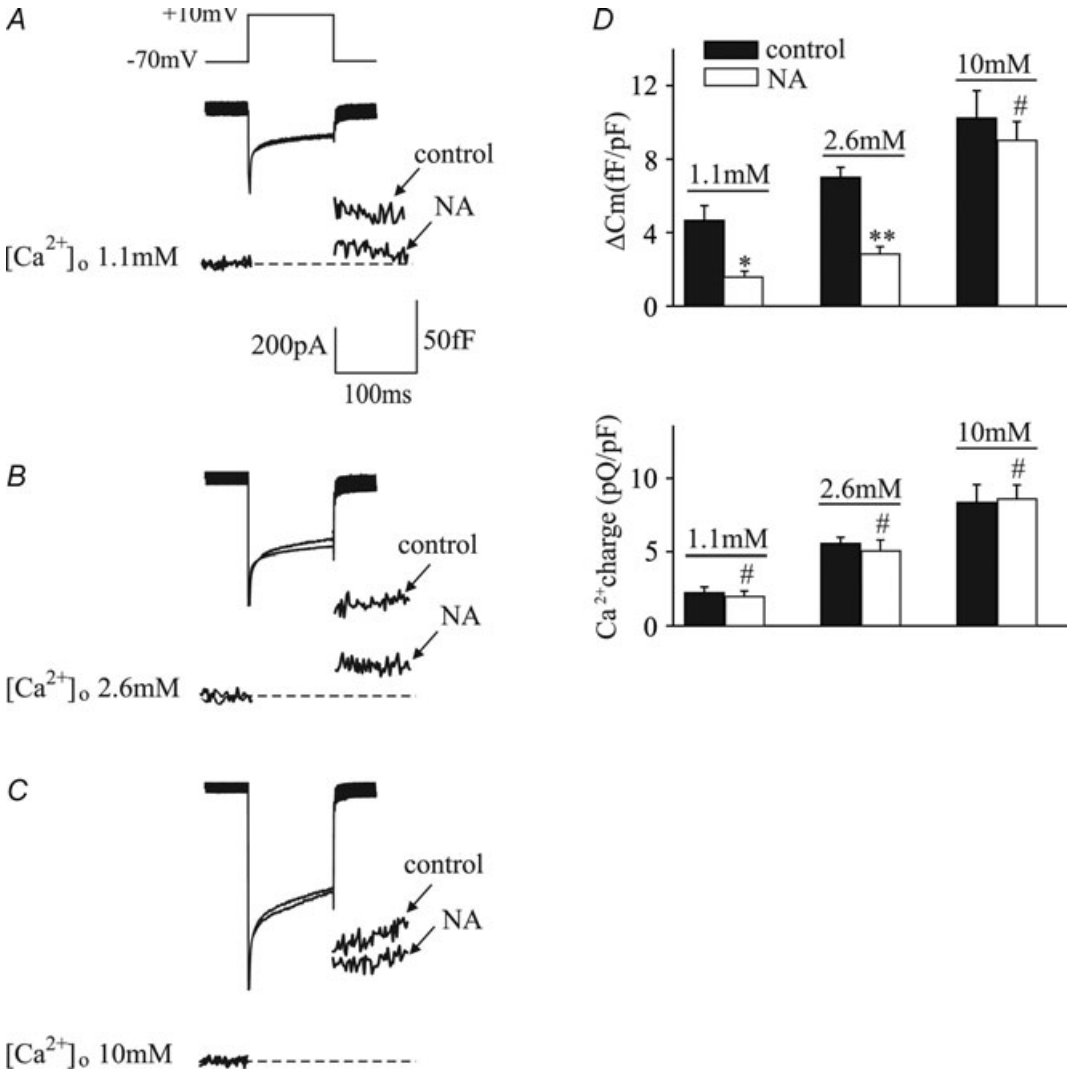

Figure 2. The inhibition of depolarization-evoked exocytosis by NA can also be abolished by increasing $[Ca^{2+}]_o$
Under the standard whole-cell configuration, the exocytosis elicited by depolarizing pulses (from −70 to +10 mV) was monitored in control and NA-treated cells. *A*, *B* and *C*, control and NA-treated cells were stimulated with 100 ms pulses at $[Ca^{2+}]_o$ of 1.1, 2.6 and 10 mM, respectively. Significant inhibition of exocytosis by NA was observed when $[Ca^{2+}]_o$ was 1.1 or 2.6 mM. The inhibition was abolished when $[Ca^{2+}]_o$ was increased to 10 mM. The data in *A*, *B* and *C* are summarized in *D*, control (filled columns) and NA (open columns). The traces shown in this figure were averaged from 11–32 cells, and the arrows indicate the different experimental conditions. The values of ΔC_m and charge integrals were normalized by cell size. $^*P < 0.05$, $^{**}P < 0.01$, #n.s.

the hypothesis that NA and mSIRK share the same signalling pathway in the regulation of exocytosis, polyclonal antibodies raised against Gβ subunits (anti-Gβ) were added to the pipette solution and dialysed into the cells. Consistent with the hypothesis, the inhibition of exocytosis in NA-treated cells was almost abolished in the presence of anti-Gβ (Fig. 4*Ba*). In contrast, polyclonal antibodies raised against Gα subunits of

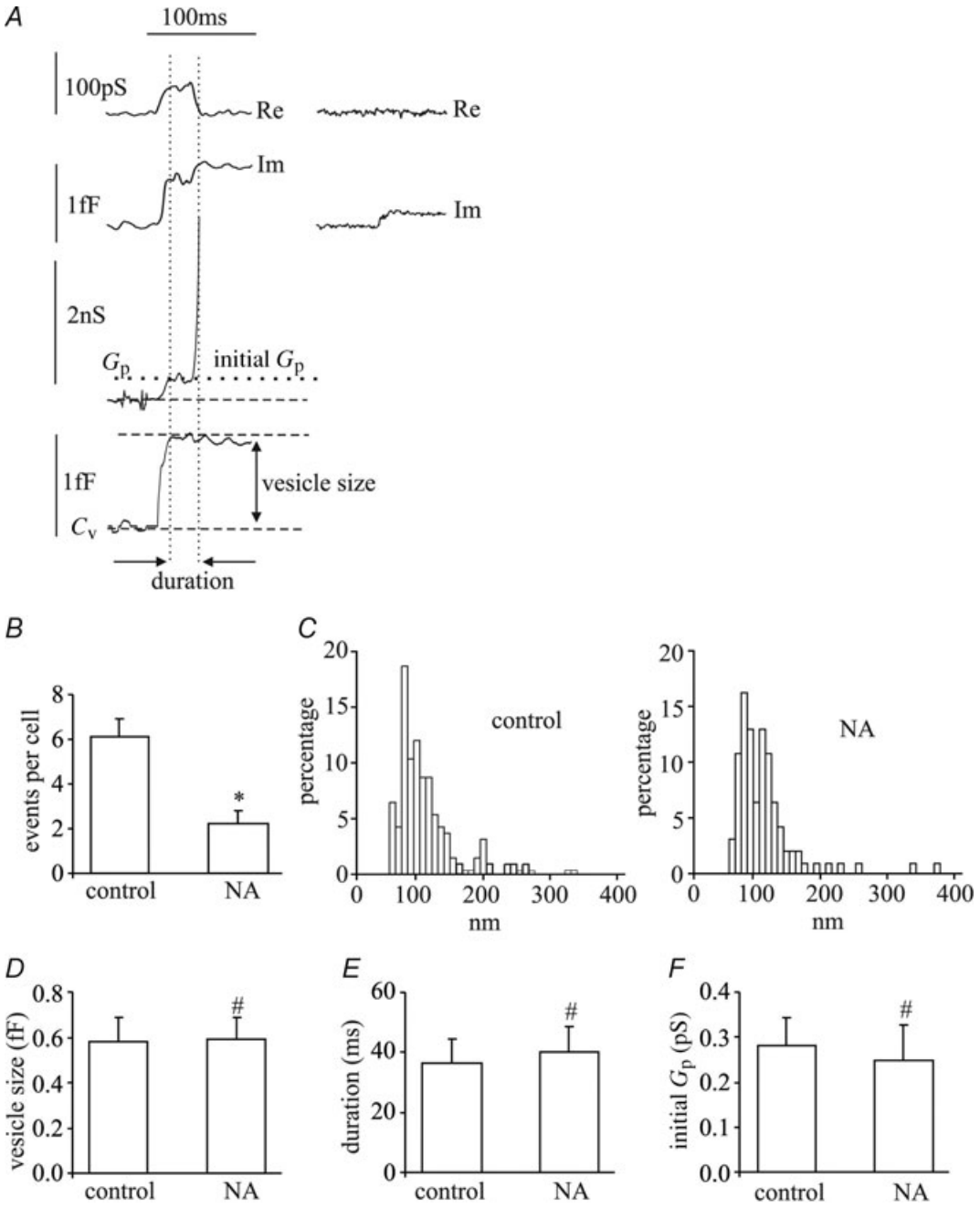

Figure 3. NA reduces the number of exocytotic events in INS-832/13 cells, without affecting vesicle size or fusion pore properties

A, two types of individual exocytotic events were detected using cell-attached capacitance measurements, the small event without detectable fusion pore conductance change (right panel), and the large event with detectable fusion pore conductance change (G_p; left panel). C_v, vesicle capacitance. *B*, summary of the number of exocytotic events occurring in control and NA-treated cells. *C* and *D*, the size distributions of exocytotic vesicles calibrated to the vesicle diameters, and the mean values of vesicle size, respectively, in control and NA-treated cells. *E* and *F*, summaries of the fusion pore duration and initial fusion pore conductance, respectively. $^*P < 0.05$, $^{**}P < 0.01$, #n.s.

heterotrimeric $G_{i,o,t,z,gust}$ proteins (anti-Gα_{common}) had no effect on the NA-induced inhibition (Fig. 4*Ba*). As summarized in Fig. 4*Bb*, the inhibition induced by NA was abolished by anti-Gβ, but neither by anti-Gα_{common} nor by other non-specific antibodies, indicating that the inhibition of exocytosis by NA is mediated by G$\beta\gamma$ subunits (control, 8.5 ± 0.6 fF pF^{-1}, $n = 41$ cells; NA+anti-Gβ, 7.5 ± 0.5 fF pF^{-1}, $n = 38$ cells, n.s.; NA+anti-Gα_{common}, 2.8 ± 0.2 fF pF^{-1}, $n = 26$ cells, $P < 0.01$; NA+anti-goat serum, 3.0 ± 0.3 fF pF^{-1}, $n = 22$ cells, $P < 0.05$; NA+anti-rabbit serum, 2.8 ± 0.3, $n = 20$ cells, $P < 0.01$). Importantly, the inhibition induced by NA and mSIRK could both be overcome, when the Ca^{2+} influx was increased by prolongation of the stimulating pulses to 500 ms (Fig. 4*Ca* and *b* control, 31.6 ± 2.2 fF pF^{-1}, $n = 34$ cells; NA, 27.4 ± 2.0 fF pF^{-1}, $n = 28$ cells, n.s.; mSIRK, 32.3 ± 2.4 fF pF^{-1}, $n = 25$ cells, n.s.) further supporting the conclusion that NA and mSIRK act by similar mechanisms.

NA inhibits Ca^{2+}-evoked exocytosis via an interaction between G$\beta\gamma$ subunits and the C-terminus of SNAP-25

The Ca^{2+}-dependent binding of synaptotagmin to the C-terminal domain of SNAP-25 is essential for Ca^{2+}-triggered exocytosis of dense core vesicles (Zhang *et al.* 2002). This binding is competitively blocked by the binding of G$\beta\gamma$ subunits to the SNARE complex (Blackmer *et al.* 2005; Gerachshenko *et al.* 2005). BoNT/A cleaves off nine amino acids at the C-terminus of SNAP-25 (Binz *et al.* 1994) rendering it incapable of interacting with synaptotagmin. When BoNT/A light chain (1 μM) was included in the pipette solution and dialysed into

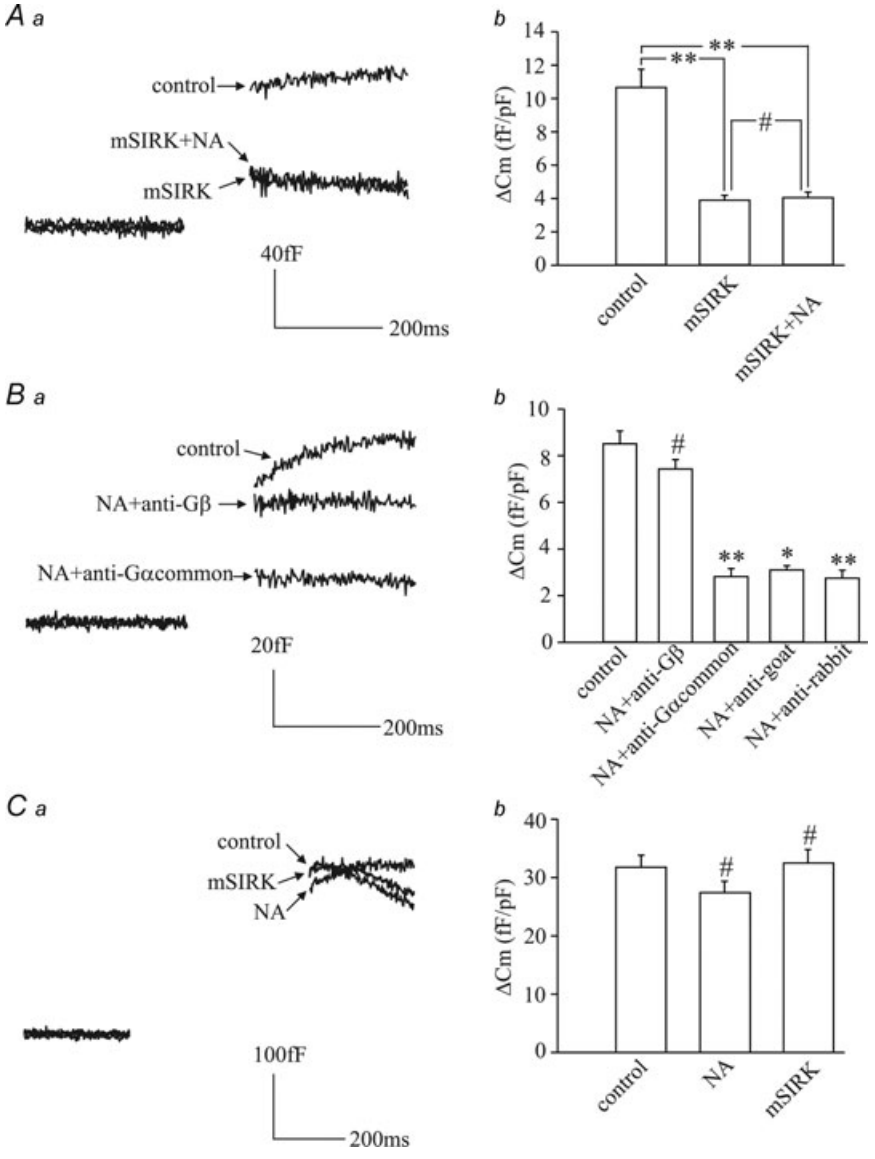

Figure 4. G$\beta\gamma$ subunits are involved in the inhibitory effect of NA on exocytosis
The stimulating protocols applied in *A* and *B* are the same as that performed in Fig. 1*A*. *A*, averaged traces of ΔC_m (*a*) recorded under the conditions indicated, and the summaries (*b*) normalized by cell size. *B*, averaged traces of ΔC_m (*a*) recorded under the conditions indicated. In the presence of NA, either anti-Gβ or anti-Gα_{common} was added to the pipette solutions. To exclude non-specific effects, anti-Gβ and anti-Gα_{common} were replaced by IgG (not shown). All the analyses are summarized in *Bb* (normalized by cell size). *C*, averaged traces of ΔC_m (*Ca*) evoked by a single 500 ms depolarizing pulse (from -70 mV to $+10$ mV) under the conditions indicated, and the summaries (*Cb*) normalized by cell size. $^*P < 0.05$, $^{**}P < 0.01$, #n.s. To exclude possible steric effects of IgG and non-specific effects of anti-Gα_{common}/anti-Gβ, the studies were controlled by testing the effects of anti-goat IgG, anti-rabbit IgG, anti-Gα_{common} and anti-Gβ alone, in the absence of NA. No effects were observed (data not shown).

the cells, exocytosis in response to a 100 ms stimulation pulse was reduced by 40% (control, 10.7 ± 0.9 fF pF^{-1}, $n = 23$ cells; BoNT/A, 6.5 ± 0.4 fF pF^{-1}, $n = 37$ cells, $P < 0.05$) but not completely abolished, consistent with other reports (Xu *et al.* 1998; Blackmer *et al.* 2005). However, when SNAP-25 was cleaved by BoNT/A, NA-induced inhibition was abolished (Fig. 5*Aa* and *b*; NA, 2.8 ± 0.2 fF pF^{-1}, $n = 33$ cells, $P < 0.01$; BoNT/A+NA, 6.8 ± 0.7 fF pF^{-1}, $n = 25$ cells, $P < 0.05$). In the presence of BoNT/A, there was no difference in exocytosis between NA-treated and -untreated cells, while BoNT/A reduced exocytosis compared to control cells. Exocytosis in BoNT/A+NA-treated cells was still higher than in cells treated with NA alone. These results indicate that G$\beta\gamma$ interacts with the C-terminus of SNAP-25 to mediate the NA-induced inhibition of exocytosis. If the C-terminus of SNAP-25 represents the target for G$\beta\gamma$, then peptides mimicking this binding region should block NA-mediated inhibition. To test this prediction, a 14 amino acid peptide containing the BoNT/A cleavage site in the C-terminus of SNAP-25 (SNAP-25$^{193-206}$, 60 μM) was added to the intracellular solution and dialysed into the cells (Fig. 5*B*). In the presence of SNAP-25$^{193-206}$, the amplitude of evoked ΔC_m was 9.2 ± 0.9 fF pF^{-1} ($n = 17$ cells), similar to that in the presence of a scrambled control peptide with the amino acids 193–206 in random order (10.2 ± 1.0 fF pF^{-1}, $n = 19$ cells) and to that of control cells (Fig. 5*Ab*). However, in the presence of SNAP-25$^{193-206}$, NA-induced inhibition was reduced to ~16% (SNAP-25$^{193-206}$+NA, 7.7 ± 0.7 fF pF^{-1}, $n = 26$ cells, $P < 0.05$), but was unchanged from its normal value when the scrambled peptide was used (Fig. 5*Bb*, NA+scrambled peptide, 3.3 ± 0.3 fF pF^{-1}, $n = 24$ cells, $P < 0.01$).

NA retards the refilling of the RRP via G$\alpha_{i1/2}$ subunits

As shown in Figs 1*A* and 5*A*, exocytosis stimulated by a single depolarizing pulse of 100 ms was inhibited by NA and the inhibition was largely abolished by anti-Gβ (Fig. 4*B*). However, when exocytosis was triggered by a pulse train, the control and NA+anti-Gβ-treated cells did still exhibit an obvious difference in ΔC_m (Fig. 6*A*), indicating that under these conditions antibodies against Gβ did not fully abolish the NA-induced inhibition of exocytosis. As shown, the amplitudes of ΔC_m elicited by the 1st pulse in control and NA+anti-Gβ-treated cells were very similar as before. However, a strong reduction of exocytosis was observed in NA+anti-Gβ-treated cells in response to the subsequent stimuli (Fig. 6*A*).

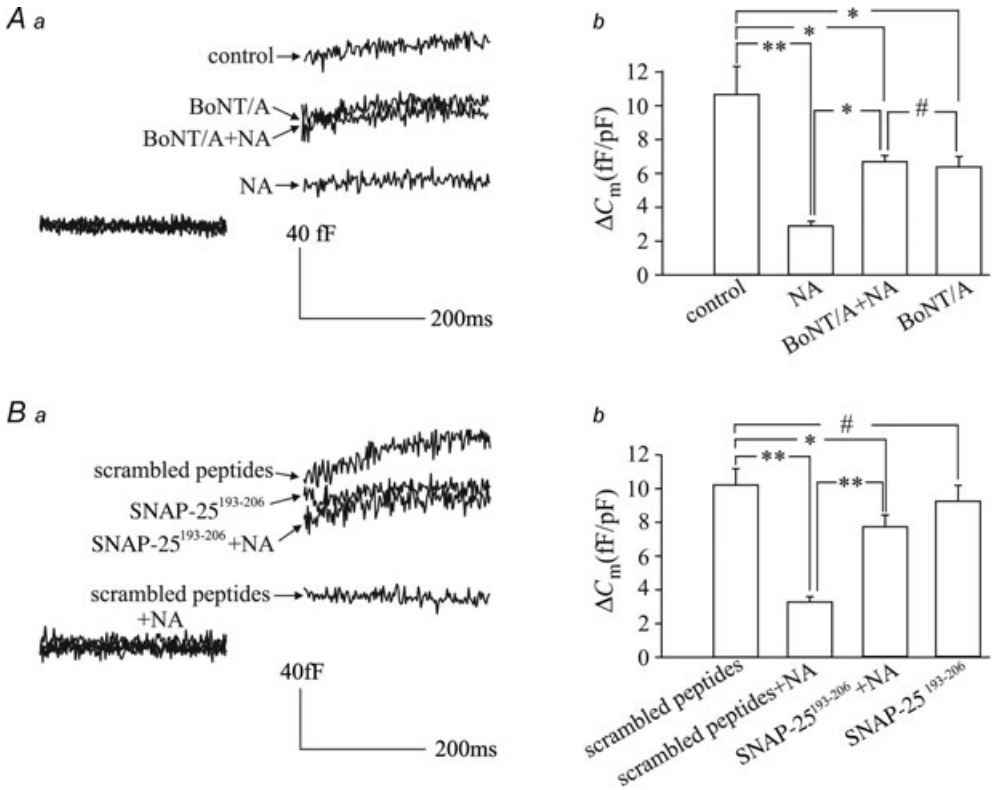

Figure 5. The inhibition of exocytosis by NA can be attenuated by BoNT/A and by a synthesized peptide mimicking the C-terminus of SNAP-25
A and *B*, the traces of ΔC_m (*Aa*, *Ba*) were measured under the conditions indicated, and the corresponding analyses (*Ab*, *Bb*) normalized by cell size. $^*P < 0.05$, $^{**}P < 0.01$, #n.s.

Only when the NA-treated cells were stimulated in the presence of both anti-Gβ and anti-Gα_{common} the capacitance trace responding to the whole pulse train closely resembled the trace in control cells. The cumulative ΔC_m, evoked by the 15 individual pulses, were added up (ΔC_{mtotal}) and quantitatively analysed in Fig. 6*B*. The average ΔC_{mtotal} in control cells was 29.1 ± 1.6 fF pF^{-1} ($n = 41$ cells) and was significantly reduced by NA in the presence of NA+anti-Gβ (17.4 ± 0.9 fF pF^{-1}, $n = 38$ cells, $P < 0.01$), and NA+anti-goat and NA+anti-rabbit groups (10.2 ± 1.0 fF pF^{-1} and 11.3 ± 1.4 fF pF^{-1}, $n = 22$ and 18 cells, respectively, $P < 0.01$ for both). In contrast, NA did not significantly inhibit cumulative exocytosis stimulated by the pulse train when both antibodies were present NA+anti-Gβ+anti-Gα_{common} (27.4 ± 2.5 fF pF^{-1}, $n = 38$ cells, n.s.). Exocytosis in response to the later pulses depends not only on stimulation and release from the RRP but also on the rate at which the RRP is refilled. To estimate the size of the RRP, we applied the dual stimulation protocol (Gillis *et al*. 1996), consisting of two 250 ms pulses separated by a 100 ms interpulse interval (Fig. 7*A*). The short interpulse interval is required to minimize refilling of the pool between the first and second stimulations. In this protocol, pool depletion due to the first stimulation (ΔC_{m1}) is manifest when the response to the second pulse (ΔC_{m2}) is small, as is the case in Fig. 7*A*. In 23 cells, the mean normalized RRP size was 34.1 ± 3.2 fF pF^{-1}. As the average exocytosis stimulated by a single 500 ms pulse was 31.6 ± 2.2 fF pF^{-1} (Fig. 1*C*), this single 500 ms depolarizing pulse is sufficient to essentially deplete the RRP in INS 832/13 cells. The fact that in NA-treated cells the ΔC_m stimulated by a 500 ms pulse was unchanged compared to controls (Fig. 4*C*) means that the size of the RRP in NA-treated cells at the start of the recordings was unchanged by the treatment.

To measure the rates of pool refilling directly, a double pulse protocol with different interpulse intervals was applied. Because a single 500 ms pulse (from −70 mV to +10 mV) is capable of depleting the RRP and abolishes the direct inhibitory effect of NA on exocytosis, the duration of the stimulation in the dual-pulse protocol was set to 500 ms. The 2nd pulse was applied after different intervals from 1 to 40 s. The ΔC_m resulting from the 1st (ΔC_{m1}) and the 2nd (ΔC_{m2}) depolarizing pulses were determined. In Fig. 7*B* the ratio of $\Delta C_{m2}/\Delta C_{m1}$ is plotted *versus* the corresponding interpulse intervals and expressed as a percentage of the initial pool size. The refilling of the RRP in control cells increased from less than 20% after 1 s to ∼90% after 40 s. In the presence of NA the refilling rate was markedly reduced such that the pool refilled only

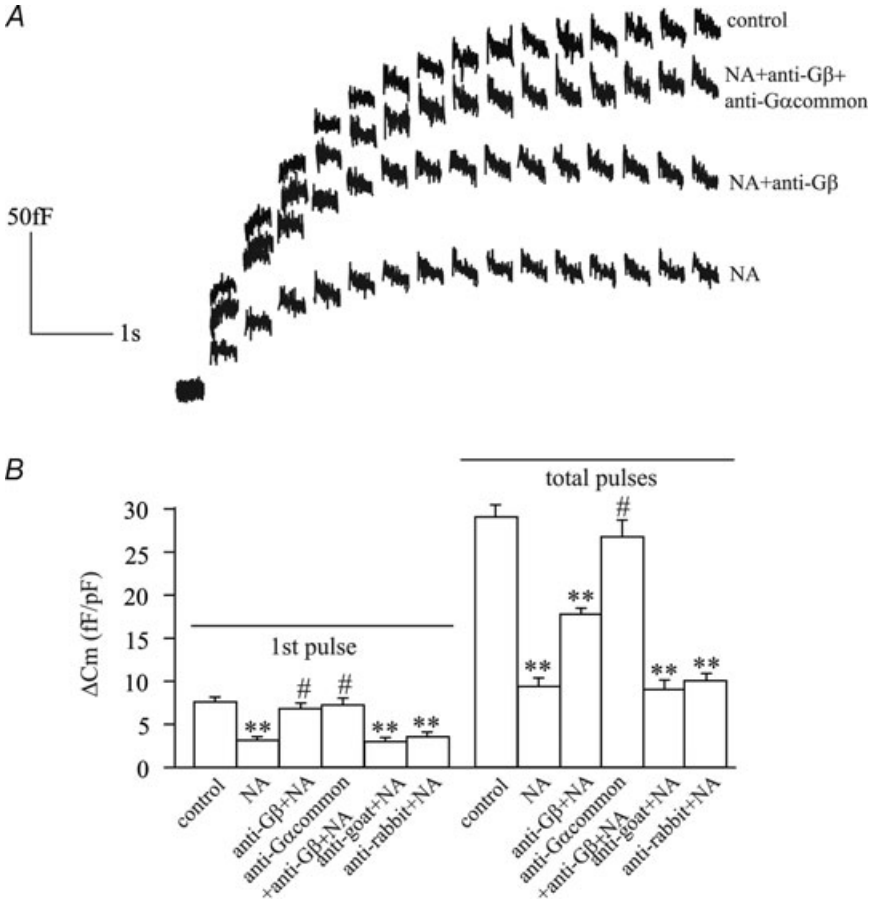

Figure 6. Effects of anti-Gβ and anti-Gα_{common} antibodies on NA-induced inhibition of exocytosis due to a depolarizing pulse chain
A, the cells in different experimental groups responded differentially to the depolarizing pulse train (100 ms pulse duration from −70 mV to +10 mV, 300 ms pulse interval). *B*, analysis of ΔC_m responses in *A* to the 1st and total pulses, respectively. To exclude possible steric effects of IgG and non-specific effects of anti-Gα_{common}/anti-Gβ, the studies were controlled by testing the effects of anti-goat IgG, anti-rabbit IgG, anti-Gα_{common} and anti-Gβ alone, in the absence of NA. No effects were observed (data not shown). Data similar to these for control and NA-treated cells were obtained when the experiments were repeated under the perforated patch configuration.

to ∼5% after 1 s and ∼50% after 40 s. To determine if NA treatment impairs the refilling of the RRP via $G\alpha_{i/o}$, synthetic peptides containing the last 11 amino acids of the α-subunits of $G_{i/o}$ proteins were tested. These peptides are known to block the interaction between G proteins and their activated receptors (Gilchrist *et al.* 2002) and we have used them successfully previously (Zhao *et al.* 2008). When the blocking peptide for $G\alpha_{i1/2}$ was included in the pipette solution the rate of recovery for NA-treated cells was similar to that of the control cells. In contrast, in the presence of the blocking peptides for $G\alpha_{o1}$, $G\alpha_{o2}$, $G\alpha_{i3}$ or the scrambled peptide G_{ir}, the recovery at each time point was similarly inhibited by NA treatment as in the absence of any peptides (Fig. 7*B*). These results show that refilling of the RRP was retarded by NA via activation of $G\alpha_{i1/2}$.

Discussion

Physiological inhibitors of insulin secretion such as NA, acting on the α_2-adrenergic receptor, have multiple effects on their target cells. These effects, exerted on ion channels, enzymes and exocytosis, were widely thought to be mediated by the PTX-sensitive heterotrimeric G_i/G_o proteins (Komatsu *et al.* 1995*a*; Sharp, 1996) until the

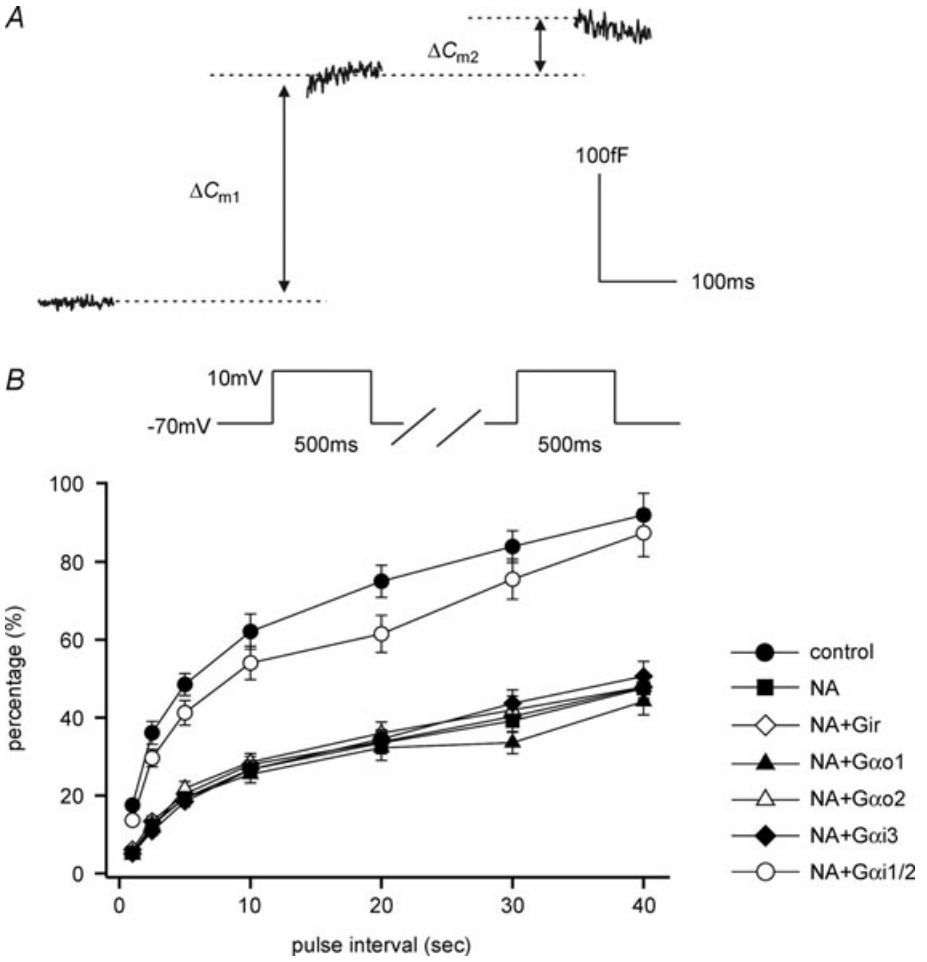

Figure 7. Measurement of the size of the RRP and its refilling rates in the presence of blocking peptides specific for the $G\alpha_i$ and $G\alpha_o$ proteins

A, the averaged capacitance traces obtained in control cells by using a dual-pulse protocol (two 250 ms pulses with an interval of 100 ms). The RRP size was estimated according to the equation, $\mathrm{RRP} = \frac{\Delta C_{m1}+\Delta C_{m2}}{1-(\frac{\Delta C_{m2}}{\Delta C_{m1}})^2}$. *B*, in different cell groups, the refilling rates of the RRP were estimated by using a dual-pulse protocol with various intervals from 1 to 40 s. The stimulatory pulses from −70 mV to +10 mV were 500 ms in duration in order to block the inhibitory effect of NA on exocytosis and to release all the granules present in the RRP. The ratios of 2nd ΔC_m /1st ΔC_m were plotted *versus* the pulse intervals, as shown. Studies were performed under control and NA-treated conditions, and under NA-treated conditions with the pipette solutions containing different blocking peptides as indicated. The scrambled peptide (Gir) was applied as a control. $^*P < 0.05$, $^{**}P < 0.01$, #n.s.

recent demonstration of PGE_1-induced inhibition of adenylyl cyclase via the PTX-insensitive G_Z (Kimple *et al.* 2008). In the endocrine pancreatic β-cell, the overall effect of NA is to inhibit stimulated insulin secretion and its potentiation by agents such as GLP-1 that act by raising cyclic AMP levels. This is achieved by activation of K^+ channels including the important K_{ATP} channel (Zhao *et al.* 2008), inhibition of adenylyl cyclase (Wiedenkeller & Sharp, 1983) and inhibition of exocytosis *per se* (Sharp, 1996). The latter is usually referred to as the distal inhibitory effect. Additionally, there are reports that in some clonal cell lines the inhibitors can directly reduce the activity of the L-type Ca^{2+} channels (Homaidan *et al.* 1991; Hsu *et al.* 1991). This has not been observed in primary β-cells, nor is it seen in the INS 832/13 cell line that we have used here. We show now that NA has two distinct distal inhibitory effects, a direct inhibition of exocytosis from the RRP and a slowing of the refilling of the RRP.

NA inhibition of exocytosis is mediated by G$\beta\gamma$/SNAP-25 interaction

The direct effect of NA to inhibit the release of insulin is due to a decreased number of exocytotic events without a change in vesicle size or fusion pore properties. This indicates that the inhibitory mechanism is exerted at a site common to the mechanisms of exocytosis of the granules following a stimulatory increase in $[Ca^{2+}]_i$. In previous studies on the distal inhibitory effect it was suggested that the inhibition was mediated by activation of the protein phosphatase calcineurin. The basis for this was that deltamethrin, a well-known inhibitor of calcineurin, blocked the inhibitory effect of somatostatin and the α_2-adrenergic agonist clonidine (Renstrom *et al.* 1996). Similarly, in the same study, a calcineurin auto-inhibitory peptide corresponding to amino acids 457–482 (the calmodulin-binding domain) blocked the inhibitory effect of somatostatin. These results suggested that the mechanism of distal inhibition was due to calcineurin-mediated dephosphorylation of a protein critical for exocytosis. However, studies on a similar distal mechanism, inhibition of neurotransmitter release downstream of elevated $[Ca^{2+}]_i$ demonstrated that G$\beta\gamma$ is involved and provided a convincing mechanism of action, i.e. G$\beta\gamma$ binding to the C-terminus of SNAP-25 and competitive blockade of the interaction between the calcium sensor protein synaptotagmin and SNAP-25 on the SNARE complex, thus inhibiting exocytosis (Blackmer *et al.* 2001, 2005; Gerachshenko *et al.* 2005). Therefore, we looked into the possibility that the same mechanism was present in the β-cell. We found that anti-Gβ antibodies blocked NA inhibition of exocytosis and also that the $\beta\gamma$-activating peptide mSIRK inhibited exocytosis to the same extent as NA. Furthermore, the combination of NA and mSIRK caused no additional inhibition relative to either of them alone and the inhibitory effects of both were overcome by increased Ca^{2+} influx. These results provide strong evidence that both NA and mSIRK act by releasing G$\beta\gamma$. Further, BoNT/A, which cleaves off the C-terminus of SNAP-25 prevented NA from inhibiting exocytosis, and a C-terminal SNAP-25 peptide, that contains the BoNT/A cleavage site also blocked the inhibitory effect of NA. These results strongly suggest that NA inhibits exocytosis by activating G$\beta\gamma$ and binding of the released G$\beta\gamma$ to the C-terminus of SNAP-25. This would be similar to the inhibition of neurotransmitter release and is not in accord with the idea that calcineurin is involved in the distal inhibition of exocytosis.

Stimulation of exocytosis in insulin-secreting cells involves not only the SNARE proteins but also synaptotagmin (Gauthier & Wollheim, 2008), complexin (Abderrahmani *et al.* 2004), and other proteins. It has recently been proposed that complexin interacts with the C-terminal part of the SNARE domains, thereby activating and also clamping the SNARE complex such that synaptotagmin can reverse the clamping function upon Ca^{2+} binding (Maximov *et al.* 2009). Release of the clamping function is followed by zippering of the SNARE domains and a force transfer to the membranes that lead to fusion. The G$\beta\gamma$ activated by NA inhibits exocytosis via its interaction with the SNAP-25 C-terminus. G$\beta\gamma$ may thus prevent complexin from activating the SNARE complex, inhibit the synaptotagmin/SNAP-25 interaction that releases the clamping function, interferes with the force transfer to the membranes, the C-terminal zippering and fusion pore formation. It seems likely that G$\beta\gamma$ could interfere with all these steps due to its binding to SNAP-25.

The inhibition of exocytosis by NA in response to a 100 ms depolarizing pulse is substantial but not complete. When exocytosis is stimulated by a 500 ms pulse, generating larger Ca^{2+} influx and extending the duration of the Ca^{2+} rise, NA-induced inhibition is abolished, as is inhibition by release of G$\beta\gamma$ by mSIRK. Thus, all the granules in the RRP can undergo exocytosis even in the presence of the released G$\beta\gamma$, if the Ca^{2+} stimulus is sufficiently high. As reported, in the presence of a very high $[Ca^{2+}]_i$, synaptotagmin is able to compete successfully with G$\beta\gamma$ for SNAP-25 (Blackmer *et al.* 2005; Gerachshenko *et al.* 2005). Fusion of a secretory vesicle involves activation of multiple SNARE complexes although the number of SNARE complexes required for a single fusion event is not known. It thus seems likely that some fraction of the available SNARE complexes is rendered inactive by G$\beta\gamma$ binding but that in response to a sufficiently large Ca^{2+} stimulus a sufficient number of SNARE complexes can still be activated by synaptotagmin such that fusion of the vesicle is fully enabled.

NA inhibits refilling of the RRP via $G\alpha_{i1/2}$

In addition to the direct inhibition of exocytosis via $G\beta\gamma$, NA retarded the rate of refilling of the RRP. This provides a possible explanation for a previous report that high Ca^{2+} influx (using 500 ms depolarizing pulses from −70 mV to 0 mV) did not block the effects of inhibitors (Renstrom *et al.* 1996) as we have observed here with a slightly larger depolarization. As their method was essentially a dual-pulse protocol (depolarization under control conditions followed by treatment with somatostatin and a second depolarization), the reduced response to somatostatin seen and interpreted as inhibition of exocytosis may reflect retardation of refilling of the granule pool after its depletion by the first pulse. The recruitment and priming of secretory granules from reserve pools into RRPs is needed to enable exocytosis to occur following discharge of the RRP (Bittner & Holz, 1992; Neher & Zucker, 1993; Straub & Sharp, 2004). The NA-induced retardation of RRP refilling is inhibited by a $G\alpha_{i1/2}$ blocking peptide but not by blocking peptides for $G\alpha_{o1}$, $G\alpha_{o2}$, $G\alpha_{i3}$ or the scrambled G_{ir}, indicating that the retardation of RRP refilling is mediated by $G\alpha_{i1}$, $G\alpha_{i2}$, or both. Regulation of the RRP size is complex. Several signalling pathways can influence the RRP, apparently by altering the rate of recruitment of vesicles. Activation of protein kinases such as cAMP-dependent protein kinase (PKA) and protein kinase C (PKC) modulate Ca^{2+}-triggered exocytosis from both primary and clonal β-cells and thus provide mechanisms for hormonal regulation of insulin release through second messengers (Ammala *et al.* 1994; Jones & Persaud, 1998; Rosengren *et al.* 2002). PKA activation potentiates insulin secretion by increasing the total number of vesicles that are available for release (Renstrom *et al.* 1997; Rorsman *et al.* 2000). PKC activation has also been linked to priming of Ca^{2+}-mediated insulin secretion (Eliasson *et al.* 1996; Efanov *et al.* 1997). PKA and PKC are also found to increase the size of a highly Ca^{2+}-sensitive vesicle pool in INS-1 cells (Yang & Gillis, 2004). The direct interactions of PKA and PKC with the secretory machinery have also been suggested in other cell types, such as chromaffin cells and hippocampal neurons, where the size of RRP and its rate of replenishment is increased (Smith *et al.* 1998; Stevens & Sullivan, 1998). As one of the mechanisms underlying NA-mediated inhibition of insulin secretion is a decrease in cAMP levels and consequent reduction of PKA activity (Sharp, 1996), it is conceivable that this could account for the retarded refilling rate. However, in our experiments, the $[cAMP]_i$ was buffered by the presence of cAMP in the intracellular (pipette) solution. Therefore, it is unlikely that $G\alpha_{i1/2}$ modified the kinetics of RRP refilling via inhibition of adenylyl cyclase (McDermott & Sharp, 1995) and interference with the cAMP–PKA signalling pathway (Kwan *et al.* 2007). While inhibition of PKC activity could be involved, there is no evidence in the literature for such an effect of NA. Similarly, while members of the Ras superfamily of GTPases also play a role in regulating the RRP (Ngsee *et al.* 1991; Bielinski *et al.* 1993; Mark *et al.* 1996; Geppert & Sudhof, 1998; Lonart & Sudhof, 2000; Polzin *et al.* 2002), there is no obvious connection to NA or $G\alpha_{i1/2}$. Thus the mechanism by which $G\alpha_{i1/2}$ impairs the refilling of the RRP remains to be elucidated.

Physiologically, it is of interest that NA inhibits both of the major pathways by which glucose induces biphasic insulin secretion. The first phase of glucose-stimulated release is due to the K_{ATP} channel-dependent or 'triggering' pathway that involves closure of K_{ATP} channels, depolarization of the β-cell, increased Ca^{2+} influx and increased $[Ca^{2+}]_i$. This is blocked by the effect of NA to activate the K_{ATP} channel and thereby re-polarize the cell (Sharp, 1996). The second phase of release is due to the K_{ATP} channel-independent or 'amplifying' pathway and is caused by an increased rate of refilling of the RRP (Straub & Sharp, 2002, 2004). We have shown here for the first time that NA retards the refilling of this pool and that this retardation is mediated by activation of $G\alpha_{i1/2}$.

In summary, NA has two distal effects that result in the inhibition of insulin secretion. One is to inhibit exocytosis by $\beta\gamma$ blockade of the binding of synaptotagmin to SNAP-25 in the SNARE complex. The other is to retard the refilling of the RRP.

References

Abderrahmani A, Niederhauser G, Plaisance V, Roehrich ME, Lenain V, Coppola T, Regazzi R & Waeber G (2004). Complexin I regulates glucose-induced secretion in pancreatic β-cells. *J Cell Sci* **117**, 2239–2247.

Ammala C, Eliasson L, Bokvist K, Berggren PO, Honkanen RE, Sjoholm A & Rorsman P (1994). Activation of protein kinases and inhibition of protein phosphatases play a central role in the regulation of exocytosis in mouse pancreatic β cells. *Proc Natl Acad Sci U S A* **91**, 4343–4347.

Bielinski DF, Pyun HY, Linko-Stentz K, Macara IG & Fine RE (1993). Ral and Rab3a are major GTP-binding proteins of axonal rapid transport and synaptic vesicles and do not redistribute following depolarization stimulated synaptosomal exocytosis. *Biochim Biophys Acta* **1151**, 246–256.

Binz T, Blasi J, Yamasaki S, Baumeister A, Link E, Südhof TC, Jahn R & Niemann H (1994). Proteolysis of SNAP-25 by types E and A botulinal neurotoxins. *J Biol Chem* **269**, 1617–1620.

Bittner MA & Holz RW (1992). Kinetic analysis of secretion from permeabilized adrenal chromaffin cells reveals distinct components. *J Biol Chem* **267**, 16219–16225.

Blackmer T, Larsen EC, Bartleson C, Kowalchyk JA, Yoon EJ, Preininger AM, Alford S, Hamm HE & Martin TFJ (2005). G protein $\beta\gamma$ directly regulates SNARE protein fusion machinery for secretory granule exocytosis. *Nat Neurosci* **8**, 421–425.

Blackmer T, Larsen EC, Takahashi M, Martin TF, Alford S & Hamm HE (2001). G protein $\beta\gamma$ subunit-mediated presynaptic inhibition: regulation of exocytotic fusion downstream of Ca^{2+} entry. *Science* **292**, 293–297.

Debus K & Lindau M (2000). Resolution of patch capacitance recordings and of fusion pore conductances in small vesicles. *Biophys J* **78**, 2983–2997.

Drews G, Debuyser A & Henquin JC (1994). Significance of membrane repolarization and cyclic AMP changes in mouse pancreatic B-cells for the inhibition of insulin release by galanin. *Mol Cell Endocrinol* **105**, 97–102.

Efanov AM, Zaitsev SV & Berggren PO (1997). Inositol hexakisphosphate stimulates non-Ca^{2+}-mediated and primes Ca^{2+}-mediated exocytosis of insulin by activation of protein kinase C. *Proc Natl Acad Sci U S A* **94**, 4435–4439.

Eliasson L, Renstrom E, Ammala C, Berggren PO, Bertorello AM, Bokvist K, Chibalin A, Deeney JT, Flatt PR, Gabel J, Gromada J, Larsson O, Lindstrom P, Rhodes CJ & Rorsman P (1996). PKC-dependent stimulation of exocytosis by sulfonylureas in pancreatic β cells. *Science* **271**, 813–815.

Fang Q, Berberian K, Gong LW, Hafez I, Sorensen JB & Lindau M (2008). The role of the C terminus of the SNARE protein SNAP-25 in fusion pore opening and a model for fusion pore mechanics. *Proc Natl Acad Sci U S A* **105**, 15388–15392.

Gauthier BR & Wollheim CB (2008). Synaptotagmins bind calcium to release insulin. *Am J Physiol Endocrinol Metab* **295**, E1279–E1286.

Geppert M & Sudhof TC (1998). RAB3 and synaptotagmin: the yin and yang of synaptic membrane fusion. *Annu Rev Neurosci* **21**, 75–95.

Gerachshenko T, Blackmer T, Yoon EJ, Bartleson C, Hamm HE & Alford S (2005). $G_{\beta\gamma}$ acts at the C terminus of SNAP-25 to mediate presynaptic inhibition. *Nat Neurosci* **8**, 597–605.

Gilchrist A, Li A & Hamm HE (2002). Gα COOH-terminal minigene vectors dissect heterotrimeric G protein signaling. *Sci STKE* **2002**, PL1.

Gillis KD, Mossner R & Neher E (1996). Protein kinase C enhances exocytosis from chromaffin cells by increasing the size of the readily releasable pool of secretory granules. *Neuron* **16**, 1209–1220.

Goubaeva F, Ghosh M, Malik S, Yang J, Hinkle PM, Griendling KK, Neubig RR & Smrcka AV (2003). Stimulation of cellular signaling and G protein subunit dissociation by G protein $\beta\gamma$ subunit-binding peptides. *J Biol Chem* **278**, 19634–19641.

Homaidan FR, Sharp GW & Nowak LM (1991). Galanin inhibits a dihydropyridine-sensitive Ca^{2+} current in the RINm5f cell line. *Proc Natl Acad Sci U S A* **88**, 8744–8748.

Hsu WH, Xiang HD, Rajan AS & Boyd AE 3rd (1991). Activation of α2-adrenergic receptors decreases Ca^{2+} influx to inhibit insulin secretion in a hamster β-cell line: an action mediated by a guanosine triphosphate-binding protein. *Endocrinology* **128**, 958–964.

Jones PM & Persaud SJ (1998). Protein kinases, protein phosphorylation, and the regulation of insulin secretion from pancreatic β-cells. *Endocr Rev* **19**, 429–461.

Katada T & Ui M (1979). Effect of *in vivo* pretreatment of rats with a new protein purified from *Bordetella* pertussis on *in vitro* secretion of insulin: role of calcium. *Endocrinology* **104**, 1822–1827.

Kimple ME, Joseph JW, Bailey CL, Fueger PT, Hendry IA, Newgard CB & Casey PJ (2008). Gαz negatively regulates insulin secretion and glucose clearance. *J Biol Chem* **283**, 4560–4567.

Komatsu M, McDermott AM, Gillison SL & Sharp GW (1995*a*). Time course of action of pertussis toxin to block the inhibition of stimulated insulin release by norepinephrine. *Endocrinology* **136**, 1857–1863.

Komatsu M, Schermerhorn T, Aizawa T & Sharp GW (1995*b*). Glucose stimulation of insulin release in the absence of extracellular Ca^{2+} and in the absence of any increase in intracellular Ca^{2+} in rat pancreatic islets. *Proc Natl Acad Sci U S A* **92**, 10728–10732.

Kwan EP, Xie L, Sheu L, Ohtsuka T & Gaisano HY (2007). Interaction between Munc13-1 and RIM is critical for glucagon-like peptide-1 mediated rescue of exocytotic defects in Munc13-1 deficient pancreatic β-cells. *Diabetes* **56**, 2579–2588.

Lang J (1999). Molecular mechanisms and regulation of insulin exocytosis as a paradigm of endocrine secretion. *Eur J Biochem* **259**, 3–17.

Lindau M & Neher E (1988). Patch-clamp techniques for time-resolved capacitance measurements in single cells. *Pflugers Arch* **411**, 137–146.

Lonart G & Sudhof TC (2000). Assembly of SNARE core complexes prior to neurotransmitter release sets the readily releasable pool of synaptic vesicles. *J Biol Chem* **275**, 27703–27707.

McDermott AM & Sharp GW (1995). Gi2 and Gi3 proteins mediate the inhibition of adenylyl cyclase by galanin in the RINm5F cell. *Diabetes* **44**, 453–459.

MacDonald PE, Eliasson L & Rorsman P (2005). Calcium increases endocytotic vesicle size and accelerates membrane fission in insulin-secreting INS-1 cells. *J Cell Sci* **118**, 5911–5920.

Mark BL, Jilkina O & Bhullar RP (1996). Association of Ral GTP-binding protein with human platelet dense granules. *Biochem Biophys Res Commun* **225**, 40–46.

Maximov A, Tang J, Yang X, Pang ZP & Sudhof TC (2009). Complexin controls the force transfer from SNARE complexes to membranes in fusion. *Science* **323**, 516–521.

Neher E & Zucker RS (1993). Multiple calcium-dependent processes related to secretion in bovine chromaffin cells. *Neuron* **10**, 21–30.

Ngsee JK, Elferink LA & Scheller RH (1991). A family of ras-like GTP-binding proteins expressed in electromotor neurons. *J Biol Chem* **266**, 2675–2680.

Polzin A, Shipitsin M, Goi T, Feig LA & Turner TJ (2002). Ral-GTPase influences the regulation of the readily releasable pool of synaptic vesicles. *Mol Cell Biol* **22**, 1714–1722.

Renstrom E, Ding WG, Bokvist K & Rorsman P (1996). Neurotransmitter-induced inhibition of exocytosis in insulin-secreting β cells by activation of calcineurin. *Neuron* **17**, 513–522.

Renstrom E, Eliasson L & Rorsman P (1997). Protein kinase A-dependent and -independent stimulation of exocytosis by cAMP in mouse pancreatic B-cells. *J Physiol* **502**, 105–118.

Rorsman P, Eliasson L, Renstrom E, Gromada J, Barg S & Gopel S (2000). The cell physiology of biphasic insulin secretion. *News Physiol Sci* **15**, 72–77.

Rosengren A, Filipsson K, Jing XJ, Reimer MK & Renstrom E (2002). Glucose dependence of insulinotropic actions of pituitary adenylate cyclase-activating polypeptide in insulin-secreting INS-1 cells. *Pflugers Arch* **444**, 556–567.

Sharp GW (1996). Mechanisms of inhibition of insulin release. *Am J Physiol Cell Physiol* **271**, C1781–C1799.

Sharp GW, Le Marchand-Brustel Y, Yada T, Russo LL, Bliss CR, Cormont M, Monge L & Van Obberghen E (1989). Galanin can inhibit insulin release by a mechanism other than membrane hyperpolarization or inhibition of adenylate cyclase. *J Biol Chem* **264**, 7302–7309.

Smith C, Moser T, Xu T & Neher E (1998). Cytosolic Ca^{2+} acts by two separate pathways to modulate the supply of release-competent vesicles in chromaffin cells. *Neuron* **20**, 1243–1253.

Stevens CF & Sullivan JM (1998). Regulation of the readily releasable vesicle pool by protein kinase C. *Neuron* **21**, 885–893.

Straub SG & Sharp GW (2002). Glucose-stimulated signaling pathways in biphasic insulin secretion. *Diabetes Metab Res Rev* **18**, 451–463.

Straub SG & Sharp GW (2004). Hypothesis: one rate-limiting step controls the magnitude of both phases of glucose-stimulated insulin secretion. *Am J Physiol Cell Physiol* **287**, C565–C571.

Wiedenkeller DE & Sharp GW (1983). Effects of forskolin on insulin release and cyclic AMP content in rat pancreatic islets. *Endocrinology* **113**, 2311–2313.

Xu T, Binz T, Niemann H & Neher E (1998). Multiple kinetic components of exocytosis distinguished by neurotoxin sensitivity. *Nat Neurosci* **1**, 192–200.

Yang Y & Gillis KD (2004). A highly Ca^{2+}-sensitive pool of granules is regulated by glucose and protein kinases in insulin-secreting INS-1 cells. *J Gen Physiol* **124**, 641–651.

Zhang X, Kim-Miller MJ, Fukuda M, Kowalchyk JA & Martin TF (2002). Ca^{2+}-dependent synaptotagmin binding to SNAP-25 is essential for Ca^{2+}-triggered exocytosis. *Neuron* **34**, 599–611.

Zhao Y, Fang Q, Straub SG & Sharp GW (2008). Both G_i and G_o heterotrimeric G proteins are required to exert the full effect of norepinephrine on the β-cell K_{ATP} channel. *J Biol Chem* **283**, 5306–5316.

Author contributions

Y.Z. and Q.F. contributed equally to this work. All authors contributed to the conception and design of the experiments and to the writing of the manuscript. They have all approved the final version for publication. The work was performed in the Department of Molecular Medicine and the School of Applied and Engineering Physics, Cornell University, Ithaca, NY 14853, USA.

Acknowledgements

This work was supported by NIH grants R01-54243 (to G.W.G.S.), R01-NS38200 (to M.L.) and a Career Development Award from the Juvenile Diabetes Foundation International (to S.G.S.).